

A Unified View on Graph Neural Networks as Graph Signal Denoising

Yao Ma

yao.ma@njit.edu

New Jersey Institute of Technology
Newark, New Jersey, USA

Xiaorui Liu

xiaorui@msu.edu

Michigan State University
East Lansing, Michigan, USA

Tong Zhao

tzhao2@nd.edu

University of Notre Dame
Notre Dame, Indiana, USA

Yozen Liu

yliu2@snap.com

Snap Inc.
Santa Monica, California, USA

Jiliang Tang

tangjili@msu.edu

Michigan State University
East Lansing, Michigan, USA

Neil Shah

nshah@snap.com

Snap Inc.
Seattle, Washington, USA

ABSTRACT

Graph Neural Networks (GNNs) have risen to prominence in learning representations for graph structured data. A single GNN layer typically consists of a feature transformation and a feature aggregation operation. The former normally uses feed-forward networks to transform features, while the latter aggregates the transformed features over the graph. Numerous recent works have proposed GNN models with different designs in the aggregation operation. In this work, we establish mathematically that the aggregation processes in a group of representative GNN models including GCN, GAT, PPNP, and APPNP can be regarded as (approximately) solving a graph denoising problem with a smoothness assumption. Such a unified view across GNNs not only provides a new perspective to understand a variety of aggregation operations but also enables us to develop a unified graph neural network framework UGNN. To demonstrate its promising potential, we instantiate a novel GNN model, ADA-UGNN, derived from UGNN, to handle graphs with adaptive smoothness across nodes. Comprehensive experiments show the effectiveness of ADA-UGNN. The implementation of ADA-UGNN is available at <https://github.com/alge24/ADA-UGNN>.

KEYWORDS

graph neural networks, graph signal denoising, semi-supervised classification

ACM Reference Format:

Yao Ma, Xiaorui Liu, Tong Zhao, Yozen Liu, Jiliang Tang, and Neil Shah. 2021. A Unified View on Graph Neural Networks as Graph Signal Denoising. In *Proceedings of ACM Conference (Conference'17)*. ACM, New York, NY, USA, 10 pages. <https://doi.org/10.1145/nnnnnnnn.nnnnnnnn>

1 INTRODUCTION

Graph Neural Networks (GNNs) have shown great capacity in learning representations for graph-structured data and thus have facilitated many down-stream tasks such as node classification [14, 15, 27, 32] and graph classification [6, 33]. As traditional neural models, a GNN model is usually composed of several stacking GNN layers. Given a graph \mathcal{G} with N nodes, a GNN layer typically contains a feature transformation and a feature aggregation operation as:

$$\text{Feature Transformation: } \mathbf{X}' = f_{\text{trans}}(\mathbf{X});$$

$$\text{Feature Aggregation: } \mathbf{H} = f_{\text{agg}}(\mathbf{X}'; \mathcal{G}); \quad (1)$$

where $\mathbf{X} \in \mathbb{R}^{N \times d_{in}}$ and $\mathbf{H} \in \mathbb{R}^{N \times d_{out}}$ denote the input and output features of the GNN layer with d_{in} and d_{out} as the corresponding dimensions, respectively. Similar to traditional neural models, non-linear activation layers are commonly added between consecutive GNN layers. The feature transformation operation $f_{\text{trans}}(\cdot)$ transforms the input of \mathbf{X} to $\mathbf{X}' \in \mathbb{R}^{N \times d_{out}}$ as its output, and the feature aggregation operation $f_{\text{agg}}(\cdot; \mathcal{G})$ updates node features by aggregating the transformed node features via the graph \mathcal{G} .

In general, different GNN models share similar feature transformations (often, a single feed-forward layer), while adopting different designs for the aggregation operation. We raise a natural question – is there an intrinsic connection among these feature aggregation operations and their assumptions? The significance of a positive answer to this question is two-fold. Firstly, it offers a new perspective to create a uniform understanding on representative aggregation operations. Secondly, it enables us to develop a general GNN framework that not only provides a unified view on multiple existing representative GNN models, but also has the potential to inspire new ones. In this paper, we aim to build the connection among feature aggregation operations of representative GNN models including GCN [14], GAT [27], PPNP and APPNP [15]. In particular, we mathematically establish that the aggregation operations in these models can be unified as the process of exactly, and sometimes approximately, addressing a graph signal denoising problem with Laplacian regularization [25]. This connection suggests that these aggregation operations share a unified goal: to ensure feature smoothness of connected nodes. With this understanding, we propose a general GNN framework, UGNN, which not only provides a straightforward, unified view for many existing aggregation operations, but also suggests various promising

Permission to make digital or hard copies of all or part of this work for personal or classroom use is granted without fee provided that copies are not made or distributed for profit or commercial advantage and that copies bear this notice and the full citation on the first page. Copyrights for components of this work owned by others than ACM must be honored. Abstracting with credit is permitted. To copy otherwise, or republish, to post on servers or to redistribute to lists, requires prior specific permission and/or a fee. Request permissions from permissions@acm.org.

Conference'17, July 2017, Washington, DC, USA

© 2021 Association for Computing Machinery.

ACM ISBN 978-x-xxxx-xxxx-x/YY/MM... \$15.00

<https://doi.org/10.1145/nnnnnnnn.nnnnnnnn>

directions to build new aggregation operations suitable for distinct applications and graph properties. To demonstrate its potential, we build an instance of UGNN called ADA-UGNN, which is suited for handling varying smoothness properties across nodes, and conduct experiments to show its effectiveness.

2 REPRESENTATIVE GRAPH NEURAL NETWORKS

In this section, we introduce notations for graphs and briefly summarize several representative GNN models. A graph can be denoted as $\mathcal{G} = \{\mathcal{V}, \mathcal{E}\}$, where \mathcal{V} and \mathcal{E} are its corresponding node and edge sets. The connections in \mathcal{G} can be represented as an adjacency matrix $\mathbf{A} \in \mathbb{R}^{N \times N}$, with N the number of nodes in the graph. The Laplacian matrix of the graph \mathcal{G} is denoted as \mathbf{L} . It is defined as $\mathbf{L} = \mathbf{D} - \mathbf{A}$, where \mathbf{D} is a diagonal degree matrix corresponding to \mathbf{A} . There are also normalized versions of the Laplacian matrix such as $\mathbf{L} = \mathbf{I} - \mathbf{D}^{-\frac{1}{2}} \mathbf{A} \mathbf{D}^{-\frac{1}{2}}$ or $\mathbf{L} = \mathbf{I} - \mathbf{D}^{-1} \mathbf{A}$. In this work, we sometimes adopt different Laplacians to establish connections between different GNNs and the graph denoising problem, clarifying in the text. In the following, we generally use $\mathbf{X} \in \mathbb{R}^{N \times d_{in}}$ and $\mathbf{H} \in \mathbb{R}^{N \times d_{out}}$ to denote input and output features of GNN layers. \mathbf{X}_i and \mathbf{H}_i are used to denote their corresponding i -th row, respectively. Next, we describe a few representative GNN models.

2.1 Graph Convolutional Networks

Following (1), a single GCN layer [14] can be written as follows:

$$\begin{aligned} \text{Feature Transformation: } \mathbf{X}' &= \mathbf{X}\mathbf{W}; \\ \text{Feature Aggregation: } \mathbf{H} &= \tilde{\mathbf{A}}\mathbf{X}', \end{aligned} \quad (2)$$

where $\mathbf{W} \in \mathbb{R}^{d_{in} \times d_{out}}$ is a feature transformation matrix, and $\tilde{\mathbf{A}}$ is a normalized adjacency matrix which includes a self-loop, defined as follows:

$$\tilde{\mathbf{A}} = \hat{\mathbf{D}}^{-\frac{1}{2}} \hat{\mathbf{A}} \hat{\mathbf{D}}^{-\frac{1}{2}}, \quad \text{with } \hat{\mathbf{A}} = \mathbf{A} + \mathbf{I}, \quad (3)$$

where $\hat{\mathbf{D}}$ is the degree matrix corresponding to $\hat{\mathbf{A}}$. In practice, multiple GCN layers can be stacked, where each layer takes the output of its previous layer as input. Non-linear activation functions are included between consecutive layers.

2.2 Graph Attention Networks

Graph Attention Networks (GAT) [27] adopts the same feature transformation operation as GCN in Eq. (2). The feature aggregation operation (written node-wise) for a node i is as:

$$\mathbf{H}_i = \sum_{j \in \tilde{\mathcal{N}}(i)} \alpha_{ij} \mathbf{X}'_j, \quad \text{with } \alpha_{ij} = \frac{\exp(e_{ij})}{\sum_{k \in \tilde{\mathcal{N}}(i)} \exp(e_{ik})}. \quad (4)$$

where $\tilde{\mathcal{N}}(i) = \mathcal{N}(i) \cup \{i\}$ denotes i 's neighbors (self-inclusive), and \mathbf{H}_i is the i -th row of \mathbf{H} , i.e. the output features of node i . In this aggregation operation, α_{ij} is a learnable attention score to differentiate the importance of distinct nodes in the neighborhood. Specifically, α_{ij} is a normalized form of e_{ij} , which is modeled as:

$$e_{ij} = \text{LeakyReLU} \left(\left[\mathbf{X}'_i \parallel \mathbf{X}'_j \right] \mathbf{a} \right) \quad (5)$$

where $[\cdot \parallel \cdot]$ denotes the concatenation operation and $\mathbf{a} \in \mathbb{R}^{2d}$ is a learnable vector. Similar to GCN, a GAT model usually consists of multiple stacked GAT layers.

2.3 Personalized Propagation of Neural Predictions

Personalized Propagation of Neural Predictions (PPNP) [15] introduces an aggregation operation based on Personalized PageRank (PPR). Specifically, the PPR matrix is defined as $\alpha(\mathbf{I} - (1 - \alpha)\tilde{\mathbf{A}})^{-1}$, where $\alpha \in (0, 1)$ is a hyper-parameter. The ij -th element of the PPR matrix specifies the influence of node i on node j . The feature transformation operation is modeled as Multi-layer Perception (MLP). The PPNP model can be written in the form of Eq. (1) as follows:

$$\begin{aligned} \text{Feature Transformation: } \mathbf{X}'_{in} &= \text{MLP}(\mathbf{X}); \\ \text{Feature Aggregation: } \mathbf{H} &= \alpha(\mathbf{I} - (1 - \alpha)\tilde{\mathbf{A}})^{-1} \mathbf{X}'. \end{aligned} \quad (6)$$

Unlike GCN and GAT, PPNP only consists of a single feature aggregation layer, but with a potentially deep feature transformation. Since the matrix inverse in Eq. (6) is costly, Klicpera et al. [15] also introduces a practical, approximated version of PPNP, called APPNP, where the aggregation operation is performed in an iterative way as:

$$\mathbf{H}^{(k)} = (1 - \alpha)\tilde{\mathbf{A}}\mathbf{H}^{(k-1)} + \alpha\mathbf{X}' \quad k = 1, \dots, K, \quad (7)$$

where $\mathbf{H}^{(0)} = \mathbf{X}'$ and $\mathbf{H}^{(K)}$ is the output of the feature aggregation operation. [15] shows that $\mathbf{X}'_{out}^{(K)}$ converges to the exact PPNP solution in Eq. (6) as K goes to infinity.

3 GNNS AS GRAPH SIGNAL DENOISING

In this section, we aim to establish the connections between the introduced GNN models and a graph signal denoising problem with Laplacian regularization.

PROBLEM 1 (GRAPH SIGNAL DENOISING). *Given a noisy signal $\mathbf{S} \in \mathbb{R}^{N \times d}$ on a graph \mathcal{G} , the goal is to recover a clean signal $\mathbf{F} \in \mathbb{R}^{N \times d}$, assumed to be smooth over \mathcal{G} , by solving the following optimization problem:*

$$\arg \min_{\mathbf{F}} \mathcal{L} = \|\mathbf{F} - \mathbf{S}\|_{\mathbf{F}}^2 + c \cdot \text{tr}(\mathbf{F}^{\top} \mathbf{L} \mathbf{F}). \quad (8)$$

The first term guides \mathbf{F} to be close to \mathbf{S} , while the second term $\text{tr}(\mathbf{F}^{\top} \mathbf{L} \mathbf{F})$ is the Laplacian regularization which guides \mathbf{F} 's smoothness over \mathcal{G} , with $c > 0$'s mediation. Assuming that we adopt the unnormalized version of Laplacian matrix with $\mathbf{L} = \mathbf{D} - \mathbf{A}$ (the adjacency matrix \mathbf{A} is assumed to be binary), the second term in Eq. (8) can be written in an edge-centric way or a node-centric way as:

$$\begin{aligned} \text{edge-centric: } c \sum_{(i,j) \in \mathcal{E}} \|\mathbf{F}_i - \mathbf{F}_j\|_2^2; \\ \text{node-centric: } \frac{1}{2} c \sum_{i \in \mathcal{V}} \sum_{j \in \tilde{\mathcal{N}}(i)} \|\mathbf{F}_i - \mathbf{F}_j\|_2^2. \end{aligned} \quad (9)$$

Clearly, from the edge-centric view, the regularization term measures the *global smoothness* of \mathbf{F} , which is small when connected nodes share similar features. On the other hand, from the node-centric view, we can view the term $\sum_{j \in \tilde{\mathcal{N}}(i)} \|\mathbf{F}_j - \mathbf{F}_i\|_2^2$ as a *local*

smoothness measure for node i as it measures the difference between node i and all its neighbors. The regularization term can then be regarded as a summation of local smoothness over all nodes. Similar formulations can also be derived to other types of Laplacian matrices.

In the following subsections, we show connections between aggregation operations in various GNN models and Problem 1.

3.1 Connection to PPNP and APPNP

Our main results linking PPNP and APPNP's to Eq. (8) are established in Theorems 1 and 2, respectively.

THEOREM 1. *When we adopt the normalized Laplacian matrix $\mathbf{L} = \mathbf{I} - \tilde{\mathbf{A}}$, with $\tilde{\mathbf{A}}$ defined in Eq. (3), the feature aggregation operation in PPNP (Eq. (6)) can be regarded as exactly solving Problem 1 with \mathbf{X}' as the input noisy signal and $c = \frac{1}{\alpha} - 1$.*

PROOF. Note that the objective in Eq. (8) is convex. Hence, the closed-form solution \mathbf{F}^* of Problem (8) can be obtained by setting its derivative to $\mathbf{0}$ as:

$$\frac{\partial \mathcal{L}}{\partial \mathbf{F}} = 2(\mathbf{F} - \mathbf{S}) + 2c\mathbf{L}\mathbf{F} = \mathbf{0} \Rightarrow \mathbf{F}^* = (\mathbf{I} + c\mathbf{L})^{-1}\mathbf{S} \quad (11)$$

Given $\mathbf{L} = \mathbf{I} - \tilde{\mathbf{A}}$, \mathbf{F}^* can be reformulated as:

$$\begin{aligned} \mathbf{F}^* &= (\mathbf{I} + c\mathbf{L})^{-1}\mathbf{S} = \left(\mathbf{I} + c(\mathbf{I} - \tilde{\mathbf{A}})\right)^{-1}\mathbf{S} \\ &= \frac{1}{1+c} \left(\mathbf{I} - \frac{c}{1+c}\tilde{\mathbf{A}}\right)^{-1}\mathbf{S} \end{aligned} \quad (12)$$

The feature aggregation operation in Eq. (6) is equivalent to the closed-form solution in Eq. (12) when we set $c = \frac{1}{\alpha} - 1$ and $\mathbf{S} = \mathbf{X}'$. This completes the proof. \square

THEOREM 2. *When we adopt the normalized Laplacian matrix $\mathbf{L} = \mathbf{I} - \tilde{\mathbf{A}}$, the feature aggregation operation in APPNP (Eq. (7)) approximately solves the graph signal denoising problem (8) by iterative gradient descent with \mathbf{X}' as the input noisy signal, $c = \frac{1}{\alpha} - 1$ and stepsize $b = \frac{1}{2+2c}$.*

PROOF. To solve the denoising problem in Eq. (8), we take iterative gradient method with the stepsize b . Specifically, the k -th step is as follows:

$$\begin{aligned} \mathbf{F}^{(k)} &\leftarrow \mathbf{F}^{(k-1)} - b \cdot \frac{\partial \mathcal{L}}{\partial \mathbf{F}} \Big|_{\mathbf{F}=\mathbf{F}^{(k-1)}} \\ &= (1 - 2b - 2bc)\mathbf{F}^{(k-1)} + 2b\mathbf{S} + 2bc\tilde{\mathbf{A}}\mathbf{F}^{(k-1)} \end{aligned} \quad (13)$$

where $\mathbf{F}^{(0)} = \mathbf{S}$. When we set the stepsize b as $\frac{1}{2+2c}$, we have the following iterative steps:

$$\mathbf{F}^{(k)} \leftarrow \frac{1}{1+c}\mathbf{S} + \frac{c}{1+c}\tilde{\mathbf{A}}\mathbf{F}^{(k-1)}, k = 1, \dots, K, \quad (14)$$

which is equivalent to the iterative aggregation operation of the APPNP in Eq. (7) with $\mathbf{S} = \mathbf{X}'$ and $c = \frac{1}{\alpha} - 1$. \square

These two connections provide a new explanation on the hyperparameter α in PPNP and APPNP from the graph signal denoising perspective. Specifically, a smaller α indicates a larger c , which means the obtained new feature matrix \mathbf{H} is enforced to be smoother over the graph.

Algorithm 1: K -layer GCN As Graph Signal Denoising

input : Node Features \mathbf{X} ; Adjacency Matrix $\tilde{\mathbf{A}}$
output : Refined Node Features \mathbf{H}

- 1 Initialize $\mathbf{X}^{(0)} \leftarrow \mathbf{X}, k \leftarrow 1$;
- 2 **while** $1 \leq k \leq K$ **do**
- 3 **(Feature Transformation)** $\mathbf{X}_f^{(k-1)} = \mathbf{X}^{(k-1)}\mathbf{W}^{(k-1)}$;
- 4 **(Feature Aggregation)** Let $\mathbf{X}_f^{(k-1)}$ be the input noisy signal of Eq. (8), i.e., $\mathbf{S} = \mathbf{X}_f$. Solve Problem (8) via one-step gradient descent as per Theorem 3 and denote the solution as $\mathbf{X}_g^{(k)}$;
- 5 **(Activation)** $\mathbf{X}^{(k)} = \sigma(\mathbf{X}_g^{(k)})$, where $\sigma(\cdot)$ denotes an activation function.;
- 6 $k \leftarrow k + 1$;
- 7 $\mathbf{H} = \mathbf{X}^{(K)}$;
- 8 **return** \mathbf{H}

3.2 Connection to GCN

Our main result is established in Theorem 3.

THEOREM 3. *When we adopt the normalized Laplacian matrix $\mathbf{L} = \mathbf{I} - \tilde{\mathbf{A}}$, the feature aggregation operation in GCN (Eq. (2)) can be regarded as solving Problem 1 using one-step gradient descent with \mathbf{X}' as the input noisy signal and stepsize $b = \frac{1}{2c}$.*

PROOF. The gradient with respect to \mathbf{F} at \mathbf{S} is $\frac{\partial \mathcal{L}}{\partial \mathbf{F}} \Big|_{\mathbf{F}=\mathbf{S}} = 2c\mathbf{L}\mathbf{S}$. Hence, one-step gradient descent for the graph signal denoising problem (8) can be described as:

$$\begin{aligned} \mathbf{F} &\leftarrow \mathbf{S} - b \frac{\partial \mathcal{L}}{\partial \mathbf{F}} \Big|_{\mathbf{F}=\mathbf{S}} = \mathbf{S} - 2bc\mathbf{L}\mathbf{S} \\ &= (1 - 2bc)\mathbf{S} + 2bc\tilde{\mathbf{A}}\mathbf{S}. \end{aligned} \quad (15)$$

When stepsize $b = \frac{1}{2c}$ and $\mathbf{S} = \mathbf{X}'$, we have $\mathbf{F} \leftarrow \tilde{\mathbf{A}}\mathbf{X}'$, which is the same as the aggregation operation of GCN. \square

With this connection, it is easy to verify that a GCN model with multiple GCN layers can be regarded as solving Problem 1 multiple times with different noisy signals as shown in Algorithm 1 (demonstrating for K -layer GCN). Specifically, in each layer, the aggregation component aims to solve Problem 1 with the transformed features as input noisy signal.

3.3 Connection to GAT

To establish the connection between graph signal denoising and GAT [27], in this subsection, we adopt an unnormalized version of the Laplacian, defined based on the adjacency matrix with self-loop $\tilde{\mathbf{A}}$, i.e. $\mathbf{L} = \tilde{\mathbf{D}} - \tilde{\mathbf{A}}$. Then, the denoising problem in Eq. (8) can be rewritten from a node-centric view as:

$$\arg \min_{\mathbf{F}} \mathcal{L} = \sum_{i \in \mathcal{V}} \|\mathbf{F}_i - \mathbf{S}_i\|_2^2 + \frac{1}{2} \sum_{i \in \mathcal{V}} c \sum_{j \in \tilde{\mathcal{N}}(i)} \|\mathbf{F}_i - \mathbf{F}_j\|_2^2, \quad (16)$$

where $\tilde{\mathcal{N}}(i) = \mathcal{N}(i) \cup \{i\}$ denotes the neighbors (self-inclusive) of node i . In Eq. (16), the constant c is shared by all nodes, which indicates that the same level of *local smoothness* is enforced to all nodes. By relaxing this assumption,

instead of a unified c as in Eq. (16), we can consider a node-dependent c_i for each node i :

$$\arg \min_{\mathbf{F}} \mathcal{L} = \sum_{i \in \mathcal{V}} \|\mathbf{F}_i - \mathbf{S}_i\|_2^2 + \frac{1}{2} \sum_{i \in \mathcal{V}} c_i \sum_{j \in \mathcal{N}(i)} \|\mathbf{F}_i - \mathbf{F}_j\|_2^2. \quad (17)$$

We next show that the aggregation operation in GAT is closely connected to an approximate solution of problem (17) with the help of Theorem 4.

THEOREM 4. *With adaptive stepsize $b_i = 1 / \sum_{j \in \mathcal{N}(i)} (c_i + c_j)$ for each node i , the process of taking one step of gradient descent from \mathbf{S} to solve Eq. (17) is as follows:*

$$\mathbf{F}_i \leftarrow \sum_{j \in \mathcal{N}(i)} b_i (c_i + c_j) \mathbf{S}_j. \quad (18)$$

PROOF. The gradient of Eq. (17) with respect to \mathbf{F} focusing on a node i can be written as:

$$\frac{\partial \mathcal{L}}{\partial \mathbf{F}_i} = 2(\mathbf{F}_i - \mathbf{S}_i) + \sum_{j \in \mathcal{N}(i)} (c_i + c_j) (\mathbf{F}_i - \mathbf{F}_j), \quad (19)$$

where c_j in the second term appears since i is also in the neighborhood of j . Then, the gradient at \mathbf{S} is $\left. \frac{\partial \mathcal{L}}{\partial \mathbf{F}_i} \right|_{\mathbf{F}=\mathbf{S}} = \sum_{j \in \mathcal{N}(i)} (c_i + c_j) (\mathbf{S}_i - \mathbf{S}_j)$.

Thus, one step of gradient descent starting from \mathbf{S} with stepsize b_i is as follows:

$$\begin{aligned} \mathbf{F}_i &\leftarrow \mathbf{S}_i - b_i \cdot \left. \frac{\partial \mathcal{L}}{\partial \mathbf{F}_i} \right|_{\mathbf{F}=\mathbf{S}} \\ &= \left(1 - b_i \sum_{j \in \mathcal{N}(i)} (c_i + c_j)\right) \mathbf{S}_i + \sum_{j \in \mathcal{N}(i)} b_i (c_i + c_j) \mathbf{S}_j \end{aligned} \quad (20)$$

Given $b_i = 1 / \sum_{j \in \mathcal{N}(i)} (c_i + c_j)$, Eq. (20) can be rewritten as

$$\mathbf{F}_i \leftarrow \sum_{j \in \mathcal{N}(i)} b_i (c_i + c_j) \mathbf{S}_j,$$

which completes the proof. \square

Eq. (18) resembles the aggregation operation of GAT in Eq. (4) if we treat $b_i (c_i + c_j)$ as the attention score α_{ij} . Note that we have $\sum_{j \in \mathcal{N}(i)} (c_i + c_j) = 1/b_i$, for all $i \in \mathcal{V}$, so, $(c_i + c_j)$ can be regarded as the unnormalized attention score and b_i as the normalization constant.

We further compare $b_i (c_i + c_j)$ with α_{ij} by investigating the formulation of e_{ij} in Eq. (5). Eq. (5) can be rewritten as:

$$e_{ij} = \text{LeakyReLU}(\mathbf{X}'_i \mathbf{a}_1 + \mathbf{X}'_j \mathbf{a}_2), \quad (21)$$

where $\mathbf{a}_1 \in \mathbb{R}^d$ and $\mathbf{a}_2 \in \mathbb{R}^d$ are learnable column vectors, which can be concatenated to form \mathbf{a} in Eq. (5). Comparing e_{ij} with $(c_i + c_j)$, we find that they take a similar form. Specifically, $\mathbf{X}'_i \mathbf{a}_1$ and $\mathbf{X}'_j \mathbf{a}_2$ can be regarded as the approximations of c_i and c_j , respectively. In this way, e_{ij} can be considered as a learnable function estimating $c_i + c_j$. Correspondingly, $b_i (c_i + c_j)$ and α_{ij} are the normalized versions of $c_i + c_j$ and e_{ij} , respectively. The difference between $b_i (c_i + c_j)$ and α_{ij} is that the normalization in Eq. (18) for $b_i (c_i + c_j)$ is achieved via summation rather than a softmax as Eq. (4) for α_{ij} . Since GAT makes the c_i and c_j learnable, they also include a non-linear activation in calculating e_{ij} . Note that similarly to multi-layer GCN illustrated in Algorithm 1, multi-layer GAT can

be also regarded as solving a series of graph denoising problems in Eq. (17).

4 UGNN: A UNIFIED GNN FRAMEWORK VIA GRAPH SIGNAL DENOISING

In the previous section, we established that the aggregation operations in PPNP, APPNP, GCN and GAT are intimately connected to the graph signal denoising problem with (generalized) Laplacian regularization (Problem 1). In particular, all their aggregation operations aim to ensure feature smoothness: either a global smoothness over the graph as in PPNP, APPNP and GCN, or a local smoothness for each node as in GAT. This understanding allows us to develop a unified aggregation operation via the following, more general denoising problem:

PROBLEM 2 (GENERALIZED GRAPH SIGNAL DENOISING PROBLEM).

$$\arg \min_{\mathbf{F}} \mathcal{L} = \|\mathbf{F} - \mathbf{S}\|_F^2 + r(\mathbf{C}, \mathbf{F}, \mathcal{G}), \quad (22)$$

where $r(\mathbf{C}, \mathbf{F}, \mathcal{G})$ denotes a flexible regularization term to enforce some prior of \mathbf{F} encoded by \mathcal{G} .

Note that we overload the notation \mathbf{C} here: it can function as a scalar (like a global constant in GCN), a vector (like node-wise constants in GAT) or even a matrix (edge-wise constants) if we want to give flexibility to each node pair. Different choices of $r(\cdot)$ imply different feature aggregation operations. Besides PPNP, APPNP, GCN and GAT, there are aggregation operations in more GNN models that can be associated with Problem 2 with different regularization terms such as PairNorm [34] and DropEdge [21]. These two recently proposed enhancements for developing deeper GNN models correspond to the following choices for $r(\mathbf{C}, \mathbf{F}, \mathcal{G})$:

$$\text{PairNorm: } \sum_{(i,j) \in \mathcal{E}} C_p \cdot \|\mathbf{F}_i - \mathbf{F}_j\|_2^2 - \sum_{(i,j) \notin \mathcal{E}} C_n \cdot \|\mathbf{F}_i - \mathbf{F}_j\|_2^2,$$

$$\text{DropEdge: } \sum_{(i,j) \in \mathcal{E}} C_{ij} \cdot \|\mathbf{F}_i - \mathbf{F}_j\|_2^2, \text{ where } C_{ij} \in \{0, 1\}.$$

For PairNorm, \mathbf{C} consists of $C_p, C_n > 0$ and the regularization term ensures connected nodes to be similar while disconnected nodes to be dissimilar. For DropEdge, \mathbf{C} is a sparse matrix having the same shape as the adjacency matrix. For each edge (i, j) , its corresponding C_{ij} is sampled from a Bernoulli distribution with mean $1 - q$, where q is a pre-defined dropout rate. The above mentioned regularization terms are all related to the Laplacian regularization. Other regularization terms can also be adopted, which may lead to novel designs of GNN layers. For example, if we aim to enforce piece-wise linearity in the clean signal, we can adopt $r(\mathbf{C}, \mathbf{F}, \mathcal{G}) = \mathbf{C} \cdot \|\mathbf{L}\mathbf{F}\|_1$ designed for trend filtering [26, 28].

With these discussions, we propose a unified framework (UGNN) to design GNN layers from the graph signal processing perspective: 1) Design a graph regularization term $r(\mathbf{C}, \mathbf{F}, \mathcal{G})$ in Problem 2 according to specific applications; 2) Feature Transformation: $\mathbf{X}' = f_{\text{trans}}(\mathbf{X})$; and 3) Feature Aggregation: Solve Problem 2 with $\mathbf{S} = \mathbf{X}'$ and the designed $r(\mathbf{C}, \mathbf{F}, \mathcal{G})$.

To demonstrate the potential of UGNN, we next introduce a new GNN model, ADA-UGNN by instantiating UGNN with $r(\mathbf{C}, \mathbf{F}, \mathcal{G})$ enforcing adaptive local smoothness across nodes.

5 ADA-UGNN: ADAPTIVE LOCAL SMOOTHING WITH UGNN

From the graph signal denoising perspective, PPNP, APPNP, and GCN enforces global smoothness by penalizing the difference with a constant C for all nodes. However, real-world graphs may consist of multiple groups of nodes which have different behaviors in connecting to similar neighbors. For example, Section 6.1 shows several graphs with varying distributions of local smoothness (as measured by label homophily): summarily, not all nodes are highly label-homophilic, and some nodes have considerably “noisier” neighborhoods than others. Moreover, as suggested by Jin et al. [13], Wu et al. [29], adversarial attacks on graphs tend to promote such label noise in graphs by connecting nodes from different classes and disconnecting nodes from the same class, rendering resultant graphs with varying local smoothness across nodes. Under these scenarios, a constant C might not be optimal, suggesting the value of adaptive (i.e. non-constant) smoothness assumptions. As shown in Section 3.3, by viewing GAT’s aggregation as a solution to regularized graph signal denoising, GAT can be regarded as adopting an adaptive C for different nodes, which facilitates adaptive local smoothness. However, in GAT, the graph denoising problem is solved by a single step of gradient descent, which might still be suboptimal. Furthermore, when modeling the local smoothness factor c_i in Eq. (18), GAT only uses features of node i as input, which may not be optimal since intuitively, understanding c_i as local smoothness, it should be intrinsically related to i ’s neighborhood. In this section, we adapt this notion directly into the UGNN framework by introducing a new regularization term, and develop a resulting GNN model (ADA-UGNN) which aims to enforce adaptive local smoothness to nodes in a different manner to GAT. We then utilize an iterative gradient descent method to approximate the optimal solution for Problem 2 with the following regularization term:

$$r(C, \mathbf{F}, \mathcal{G}) = \frac{1}{2} \sum_{i \in \mathcal{V}} C_i \sum_{j \in \mathcal{N}(i)} \left\| \frac{\mathbf{F}_i}{\sqrt{d_i}} - \frac{\mathbf{F}_j}{\sqrt{d_j}} \right\|_2^2 \quad (23)$$

where d_i, d_j denote the degree of nodes i and j respectively, and C_i indicates the smoothness factor of node i , which is assumed to be a fixed scalar. Note that, the above regularization term can be regarded as a generalized version of the regularization term used in PPNP, APPNP, and GCN. Similar to PPNP and APPNP, ADA-UGNN only consists of a single GNN layer. We next describe the feature transformation and aggregation operations of ADA-UGNN, and show how to derive the model via UGNN.

5.1 Feature Transformation

Similar to PPNP and APPNP, we adopt MLP for the feature transformation. Specifically, for a node classification task, the dimension of the output of the feature transformation \mathbf{X}' is the number of classes in the graph.

5.2 Feature Aggregation

We use iterative gradient descent to solve Problem 2 with the regularization term in Eq. (23). The iterative gradient descent steps are stated in the following theorem.

THEOREM 5. *With adaptive stepsize $b_i = 1/\left(2 + \sum_{j \in \mathcal{N}(i)} (C_i + C_j)/d_i\right)$ for each node i , the iterative gradient descent steps to solve Problem 2 with the regularization term in Eq. (23) is as follows:*

$$\mathbf{F}_i^{(k)} \leftarrow 2b_i \mathbf{S}_i + b_i \sum_{j \in \mathcal{N}(i)} (C_i + C_j) \frac{\mathbf{F}_j^{(k-1)}}{\sqrt{d_i d_j}}; \quad k = 1, \dots, \quad (24)$$

where $\mathbf{F}_i^{(0)} = \mathbf{S}_i$.

PROOF. The gradient of the optimization problem 2 with the regularization term in Eq. (23) with respect to \mathbf{F} (focusing on node i) is as follows:

$$\frac{\partial \mathcal{L}}{\partial \mathbf{F}_i} = 2(\mathbf{F}_i - \mathbf{S}_i) + \sum_{v_j \in \mathcal{N}(v_i)} \frac{C_i + C_j}{\sqrt{d_i}} \left(\frac{\mathbf{F}_i}{\sqrt{d_i}} - \frac{\mathbf{F}_j}{\sqrt{d_j}} \right), \quad (25)$$

where C_j in the second term appears since node i is also in the neighborhood of node j . The iterative gradient descent steps with adaptive stepsize b_i can be formulated as follows:

$$\mathbf{F}_i^{(k)} \leftarrow \mathbf{F}_i^{(k-1)} - b_i \cdot \frac{\partial \mathcal{L}}{\partial \mathbf{F}_i} \Big|_{\mathbf{F}_i = \mathbf{F}_i^{(k-1)}}; \quad k = 1, \dots \quad (26)$$

With the gradient in Eq. (25), the iterative steps in Eq. (26) can be rewritten as:

$$\begin{aligned} \mathbf{F}_i^{(k)} &\leftarrow (1 - 2b_i - b_i \sum_{v_j \in \mathcal{N}(v_i)} \frac{C_i + C_j}{d_i}) \mathbf{F}_i^{(k-1)} + 2b_i \mathbf{S}_i \\ &\quad + b_i \sum_{v_j \in \mathcal{N}(v_i)} (C_i + C_j) \frac{\mathbf{F}_j^{(k-1)}}{\sqrt{d_i d_j}}; \quad k = 1, \dots \end{aligned} \quad (27)$$

Given $b_i = 1/\left(2 + \sum_{v_j \in \mathcal{N}(v_i)} (C_i + C_j)/d_i\right)$, the iterative steps in Eq. (27) can be re-written as follows:

$$\mathbf{F}_i^{(k)} \leftarrow 2b_i \mathbf{S}_i + b_i \sum_{v_j \in \mathcal{N}(v_i)} (C_i + C_j) \frac{\mathbf{F}_j^{(k-1)}}{\sqrt{d_i d_j}}; \quad k = 1, \dots, \quad (28)$$

with $\mathbf{F}_i^{(0)} = \mathbf{S}_i$, which completes the proof. \square

Following the iterative solution in Eq. (24), we model the aggregation operation (for node i) for ADA-UGNN as:

$$\mathbf{H}_i^{(k)} \leftarrow 2b_i \mathbf{X}'_i + b_i \sum_{v_j \in \mathcal{N}(v_i)} (C_i + C_j) \frac{\mathbf{H}_j^{(k-1)}}{\sqrt{d_i d_j}}; \quad k = 1, \dots, K, \quad (29)$$

where \mathbf{X}' is the output of feature transformation, $\mathbf{H}^{(0)} = \mathbf{X}'$, K is the number gradient descent iterations, C_i can be considered as a positive scalar to control the level of “local smoothness” for node i , and b_i can be calculated from $\{C_j | j \in \mathcal{N}(i)\}$ as $b_i = 1/\left(2 + \sum_{j \in \mathcal{N}(i)} (C_i + C_j)/d_i\right)$. However, in practice, C_i is usually unknown. One possible solution is to treat C_i as hyper-parameters. But, treating C_i as hyper-parameters for all nodes is impractical, since there are in total N of them and we do not have their prior

knowledge. Thus, we instead parameterize C_i as a function of the information of the neighborhood of node i as follows:

$$C_i = s \cdot \sigma \left(h_1 \left(h_2 \left(\left\{ X'_j \mid j \in \tilde{\mathcal{N}}(i) \right\} \right) \right) \right), \quad (30)$$

where $h_2(\cdot)$ is a function to transform the neighborhood information of node i to a vector, while $h_1(\cdot)$ further transforms it to a scalar. $\sigma(\cdot)$ denotes the sigmoid function, which maps the output scalar from $h_1(\cdot)$ to $(0, 1)$ and s can be treated as a hyper-parameter controlling the upper bound of C_i . $h_1(\cdot)$ can be modeled as a single layer fully-connected neural network. There are different designs for $h_2(\cdot)$ such as channel-wise mean or variance [5]. In this paper, we adopt channel-wise variance as the $h_2(\cdot)$ function (as a measure of diversity). APPNP can be regarded a special case of ADA-UGNN, where $\sigma(h_1(h_2(\{x'_j \mid j \in \tilde{\mathcal{N}}(i)\})))$ produces a constant 1 (i.e. $C_i = s$) for all nodes. For the node classification task, the representation $\mathbf{H}^{(K)}$, which is obtained after K iterations as in Eq. (29), is directly softmax normalized row-wisely and its i -th row indicates the discrete class distribution of node i .

6 EXPERIMENTAL EVALUATION

Although our contributions in this work are primarily towards mathematical understanding and unification of GNNs, in this section, we experimentally evaluate our proposed ADA-UGNN to demonstrate the promise of deriving new aggregations as solutions of denoising problems (not in striving for state-of-the-art GNN performance). We begin with node classification experiments on standard graphs. Next, we demonstrate the effectiveness of the proposed ADA-UGNN in handling adaptive smoothness as manifested via adversarial attacks.

6.1 Node Classification

We first introduce the datasets and experimental settings in Section 6.1.1 and then present the results in Section 6.1.2.

6.1.1 Datasets and Experimental Settings. Datasets. We use 10 datasets from various domains including citation, social, co-authorship and co-purchase networks. Specifically, we use three citation networks including CORA, CITESEER, and PUBMED [22]; two social networks including BLOGCATALOG and FLICKR [12]; two co-authorship networks including COAUTHOR-CS and COAUTHOR-PH [24]; one transportation network, AIR-USA [30]; and two co-purchase networks including AMAZON-COMP and Amazon Photos [24]. We provided detailed description of these datasets as follows.

- **Citation Networks:** CORA, CITESEER and PUBMED are widely adopted benchmarks of GNN models. In these graphs, nodes represent documents and edges denote the citation links between them. Each node is associated bag-of-words features of its corresponding document and also a label indicating the research field of the document.
- **Co-purchase Graph:** AMAZON-COMP and AMAZON-PHOTO are co-purchase graphs, where nodes represent items and edges indicate that two items are frequently bought together. Each item is associated with bag-of-words features extract from its corresponding reviews. The labels of items are given by the category of them.

	#Nodes	#Edges	#Labels	#Features
CORA	2708	13264	7	1433
CITESEER	3327	12431	6	3703
PUBMED	19717	108365	3	500
AMAZON-COMP	13381	504937	10	767
AMAZON-PHOTO	7487	245573	8	745
COAUTHOR-CS	18333	182121	15	6805
COAUTHOR-PH	34493	530417	5	8415
BLOGCATALOG	5196	348682	6	8189
FLICKR	7575	487051	9	12047
AIR-USA	1190	28388	4	238

Table 1: Dataset summary statistics.

- **Co-authorship Graphs:** COAUTHOR-CS and COAUTHOR-PH are co-authorship graphs, where nodes are authors and edges indicating the co-authorship between authors. Each author is associated with some features representing the keywords of his/her papers. The label of an author indicates the his/her most active research field.
- **Blogcatalog:** BLOGCATALOG is an online blogging community where bloggers can follow each other. The BLOGCATALOG graph consists of blogger as nodes while their social relations as edges. Each blogger is associated with some features generated from key words of his/her blogs. The bloggers are labeled according to their interests.
- **Flickr:** FLICKR is an image sharing platform. The FLICKR graph consists users as its nodes and the following relation among users as its edges. The users are labeled with the groups they joined.
- **Air-USA:** AIR-USA is a air traffic graph, where each node is an airport in the US. Two nodes are considered as connected if there existing commercial flights between them. Nodes are labeled with the the passenger flow of each airport.

Some statistics about these datasets can be found in Table 1. To provide a sense of the local smoothness properties of these datasets, in addition to the summary statistics, we also illustrate the *local label smoothness* distributions in Figure 1: here, we define the local label smoothness of a node as the ratio of nodes in its neighborhood that share the same label with it. Specifically, for a node v_i we formally define the local label smoothness as follows

$$ls(i) = \frac{\sum_{j \in \mathcal{N}(i)} \mathbf{1}\{l(i) = l(j)\}}{|\mathcal{N}(i)|} \quad (31)$$

where $l(v_i)$ denotes the label of node v_i and $\mathbf{1}\{a\}$ is an indicator function, which takes 1 as output only when a is true, otherwise 0. Notably, as shown in Figure 1, the large variety in local label smoothness within several real-world datasets including BLOGCATALOG, FLICKR and AIR-USA – also observed in [4, 16, 20, 23, 36, 37] – clearly motivates the importance of the adaptive smoothness assumption in ADA-UGNN.

Experimental Settings. For the citation networks, we use the standard split as provided in Kipf and Welling [14], Yang et al. [31]. For BLOGCATALOG, FLICKR and AIR-USA, we adopt the split provided in Zhao et al. [35]. For the citation networks, social networks and transportation network, we report results averaged across 30

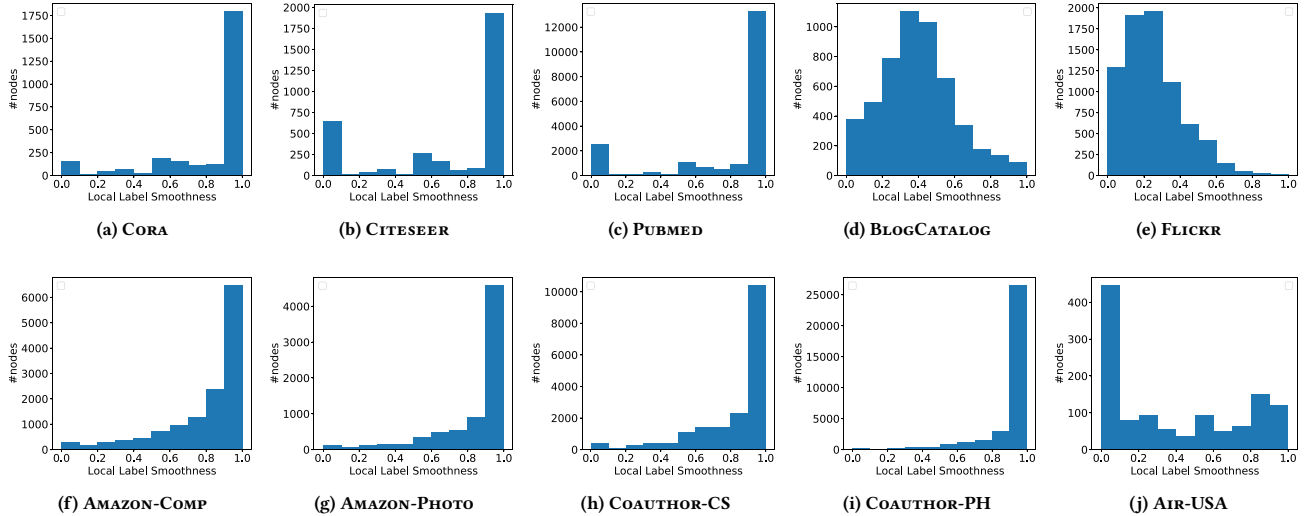


Figure 1: Distribution of local label smoothness (homophily) on different graph datasets: note the non-homogeneity of smoothness values.

Table 2: Node classification accuracy across datasets.

Accuracy (%)	GCN	GAT	APPNP	ADA-UGNN
CORA	81.75±0.8	82.56±0.8	84.49±0.6	84.79±0.7*
CITeseer	70.13±1.0	70.77±0.8	71.97±0.6	72.17±0.6
PUBMED	78.56±0.5	78.88±0.5	80.00±0.4	80.52±0.6***
AMAZON-COMP	82.79±1.3	83.01±1.5	82.99±1.6	83.40±1.3***
AMAZON-PHOTO	89.60±1.5	90.33±1.2	91.38±1.2	91.44±1.2
COAUTHOR-CS	91.55±0.6	90.95±0.7	91.69±0.4	92.33±0.5***
COAUTHOR-PH	93.23±0.7	92.86±0.7	93.84±0.5	93.92±0.6
BLOGCATALOG	71.38±2.7	72.90±1.2	92.43±0.9	93.33±0.3***
FLICKR	63.28± 0.3	52.17±1.0	83.19±0.4	84.15±0.4***
AIR-USA	56.62± 1.1	55.81± 1.7	56.20±1.2	57.32±1.2***

*, ***, ** indicate the improvement over APPNP is significant at $p < 0.1$ and 0.005

random seeds. For co-authorship and co-purchase networks, we utilize 20 labels per class for training, 30 nodes per class for validation and the remaining nodes for test. This process is repeated 20 times, which results in 20 different training/validation/test splits. For each split, the experiment is repeated for 20 times with different initialization. The average results over 20×20 experiments are reported. We compare our methods with the methods introduced in Section 2 including GCN, GAT and APPNP (we do not include PPNP due to scaling difficulty given the matrix inverse in Eq. (6)). For all methods, we tune the hyperparameters from the following options: 1) learning rate: $\{0.005, 0.01, 0.05\}$; 2) weight decay $\{5e-04, 5e-05, 5e-06, 5e-07, 5e-08\}$; and 3) dropout rate: $\{0.2, 0.5, 0.8\}$. For APPNP and our method ADA-UGNN, we further tune the number of iterations K and the upper bound s for c_i in Eq. (30) from the following range: 1) K : $\{2, 5, 10\}$; and s : $\{1, 9, 19, 29\}$. Note that we treat APPNP as a special case of our proposed method with $C_i = s$ in Eq. (30).

6.1.2 Performance Comparison. We show results in Table 2, using two-sample t -test to evaluate significance. We note a few main

observations: 1) GAT outperforms GCN in most datasets, indicating that modeling adaptive local smoothness is generally helpful; 2) APPNP/ADA-UGNN outperform GCN/GAT in most settings, suggesting iterative gradient descent offers advantages to single-step gradients, due to improved ability to achieve a denoising solution closer to the optimal; and 3) Most notably, our proposed ADA-UGNN achieves consistently better performance than GCN/GAT, and outperforms or matches APPNP across datasets. Outperformance of GAT suggests the importance of considering neighborhood information in learning local smoothness, while outperformance of APPNP suggests that adaptive local smoothness is advantaged versus fixed smoothness assumptions.

We note that APPNP is the closest contending method. However, our reported averaged results consistently outperform it, and especially so on datasets where the the local label smoothness varies a lot across nodes, like BLOGCATALOG, FLICKR, and AIR-USA. In addition to these datasets, ADA-UGNN also achieves strongly significant improvements ($p < 0.005$) over APPNP on some datasets with lesser label smoothness diversity like COAUTHOR-CS, AMAZON-COMP and PUBMED, and less significant improvements ($p < 0.1$) on CORA. Comparatively, for datasets with extremely skewed local label smoothness distributions, where the majority of nodes have perfect, 1.0 label homophily (see Figure 1) like AMAZON-PHOTO, COAUTHOR-PH, and CITESEER, improvement over APPNP is marginal. APPNP shines in such cases, since its assumption of $\sigma(h_1(h_2(\{X_j | j \in \tilde{N}(i)\}))) = 1$ is ideal for these nodes (designating maximal local smoothness). Conversely, our model has the challenging task of learning $h_1(\cdot)$ and $h_2(\cdot)$ – in such skewed cases, learning these functions may be relatively unfruitful, but still achieves strong performance. Overall, ADA-UGNN can work well no matter whether the given graph has a skewed or diverse local label smoothness distribution, but especially shines when the local label smoothness is diverse.

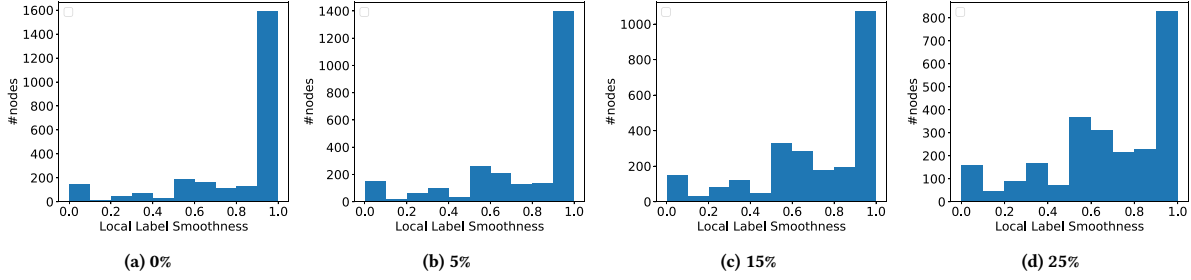


Figure 2: Distribution of local label smoothness on CORA with various attack perturbation rates.

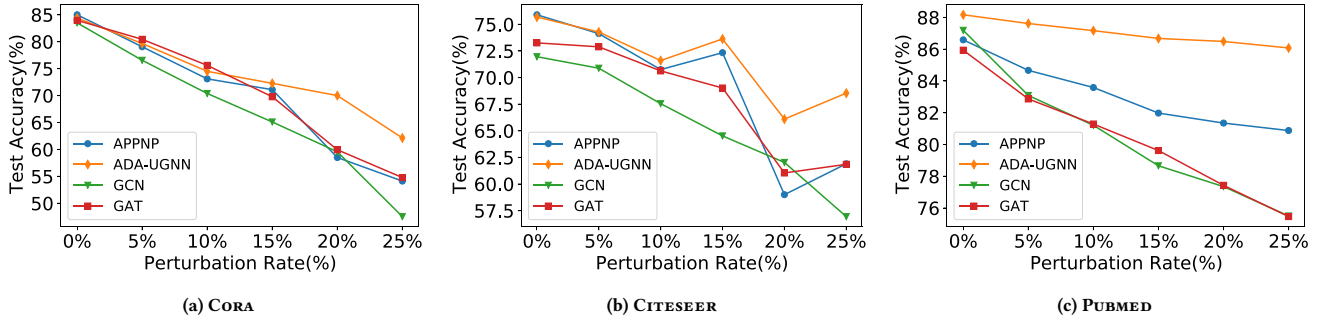


Figure 3: Node classification accuracy under adversarial attacks. The proposed ADA-UGNN maintains consistently strong performance even under high attack scale via its adaptive smoothness assumptions, where other methods degrade more quickly.

Table 3: Node classification accuracy, split across nodes with low/high local label smoothness.

Accuracy (%)	Low		High	
	APPNP	ADA-UGNN	APPNP	ADA-UGNN
CORA	38.40	40.17	90.65	90.76
CITSEER	34.20	34.83	82.00	81.90
PUBMED	41.08	44.44	88.32	88.33
AMAZON-COMP	44.08	45.81	88.08	88.31
AMAZON-PHOTO	44.57	44.94	95.61	95.54
COAUTHOR-CS	43.94	51.79	96.31	96.26
COAUTHOR-PH	37.97	43.24	96.10	95.98
BLOGCATALOG	89.70	91.15	99.49	99.06
FLICKR	81.83	82.95	96.63	96.04
AIR-USA	42.44	43.62	77.03	78.01

6.1.3 *Performance vs. Local Label Smoothness.* To further investigate how ADA-UGNN works, we partition the nodes in the test set of each dataset into two groups: (1) *high smoothness*: those with local label smoothness >0.5 , and (2) *low smoothness*: those with ≤ 0.5 , and evaluate accuracy for APPNP and the proposed ADA-UGNN for each group. The results for all datasets are shown in Table 3. Clearly, the proposed ADA-UGNN consistently improves the performance for low-smoothness nodes in most datasets, while keeping comparable performance for high-smoothness nodes. Hence, for graphs where many nodes have low-level smoothness (like BLOGCATALOG, FLICKR or AIR-USA), ADA-UGNN outperforms APPNP significantly in terms

of overall performance. However, for graphs with very few low-smoothness nodes such as COAUTHOR-PH, though ADA-UGNN still significantly improves the performance over APPNP for those low smoothness nodes, the overall performance is similar to APPNP.

6.2 Robustness Under Adversarial Attacks

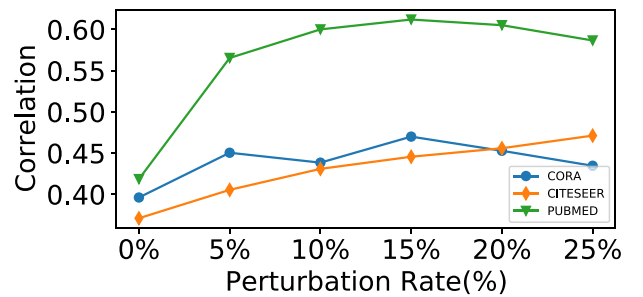


Figure 4: Correlation between ADA-UGNN’s learned C_i scores and local label smoothness.

Adversarial attacks on graphs tend to connect nodes from different classes and remove edges between nodes from the same class [13, 29], producing graphs with varying local label smoothness after attack. To further demonstrate that ADA-UGNN can handle graphs with varying local label smoothness better than alternatives,

we conduct experiments to show its robustness under adversarial attacks. Specifically, we adopt Mettack [39] to perform the attacks. We utilize the attacked graphs (5%-25% perturb rate) from Jin et al. [13] and follow the same setting, i.e. report average performance of each method over 10 random seeds. These attacked graphs are generated from CORA, CITESEER and PUBMED. As per prior work, we use only the largest connected component in each graph, and fix a 10/10/80 training, validation and test split. Hence, the results in this section are not comparable with those in the previous section. We present the local smoothness distributions of the graphs generated by Mettack [39] with different perturbation rate for CORA in Figure 2. The change in local smoothness distributions for CITESEER and PUBMED dataset are similar to CORA. We compare ADA-UGNN with GCN, GAT and APPNP. Results under varying perturbation rates (attack intensities) are shown in Figure 3, with ADA-UGNN in orange. We have the following observations: 1) ADA-UGNN is more stable than all three baselines, with the most graceful performance degradation under attack; and 2) ADA-UGNN (orange) substantially outperforms APPNP by a large margin, especially in scenarios with high perturbation rate.

These results further demonstrate that ADA-UGNN can handle graphs with varying local label smoothness better than alternatives. Note that compared to the next-best contender (APPNP), ADA-UGNN only introduces a constant number of additional parameters for modeling $h_1(\cdot)$ in Eq. (30). Although ADA-UGNN is not specifically designed to defend against adversarial attacks (and we do not claim it is the most suitable).

6.2.1 Learning Smoothness under Attack. We investigate how ADA-UGNN learns adaptive C_i under different attack perturbation ratios. Ideally, for nodes with high local label smoothness, we expect the learned C_i to be larger, such that a higher-level local smoothness is enforced to this node during model training. We consider the Pearson correlation between the learned C_i for all nodes with their local label smoothness (unknown during training). The correlation coefficients for the three datasets under various perturbation ratios are shown in Figure 4. In general, the learned C_i are strongly positively correlated with the local label smoothness under all settings on all three datasets. Moreover, compared with the clean graph (0% perturbation), the correlation scores are generally higher when the graphs are increasingly perturbed. This is likely because all the three datasets have highly skewed local label smoothness distributions as discussed in Section 6.1.2. Under perturbation, the label smoothness distributions of these three datasets become much more diverse (see Figure 2 for a demonstration), which facilitates ADA-UGNN to learn better C_i . These findings are consistent with our original conjecture in Section 6.1.2. This also partially explains why ADA-UGNN strongly outperforms APPNP under the attack setting on these datasets, compared to marginal outperformance under the clean graph setting.

7 RELATED WORKS

There are mainly two streams of work in designing GNN models, i.e. spectral-based and spatial-based. When designing spectral-based GNNs, graph convolution [25], defined based on spectral theory, is utilized to design GNN layers together with the feature transformation [1, 6, 11]. These spectral-based graph convolutions are tightly

related with graph signal processing, and they can be regarded as graph filters. Low-pass graph filters can usually be adopted to denoise graph signals [3]. In fact, most algorithms discussed in our work can be regarded as low-pass graph filters. With the emergence of GCN [14], which can be regarded as a spectral-based and also a spatial-based graph convolution operator, numerous spatial-based GNN models have since been developed [8–10, 18, 27]. A more comprehensive introduction on GNNs can be found at [17].

Graph signal denoising aims to infer a clean graph signal given a noisy one, and can be usually formulated as a graph regularized optimization problem [3]. Recently, several works connect GCN with graph signal denoising with Laplacian regularization [19, 34], finding the aggregation process in GCN models can be regarded as a first-order approximation of the optimal solution. On the other hand, GNNs are also utilized to develop novel algorithms for graph denoising [2]. Unlike these works, our paper details how a family of GNN models can be unified with a graph signal denoising perspective, and shows its promise for new architecture design.

We noticed that one concurrent work very recently released to arXiv [38], which finds optimization commonalities between some GNN models. We approach our unified framework with signal denoising, which provides a better explanation of the framework and offers a new perspective. Furthermore, our observation of the adaptive local smoothness allows us to unify GAT into our framework, and propose a new GNN model ADA-UGNN. Also, there is another concurrent work [7] connecting GNNs with graph signal denoising problem. Compared with it, our work connects diverse other models including GAT, PPNP, APPNP, DropEdge and Pairnorm with graph signal denoising problem, via UGNN’s *regularization-focused* paradigm and provides a novel connection to GAT from a local label smoothness angle.

8 CONCLUSION

In this paper, we show how various representative GNN models including GCN, PPNP, APPNP and GAT can be unified mathematically as natural instances of graph denoising problems. Specifically, the aggregation operations in these models can be regarded as exactly or approximately addressing such denoising problems. With these observations, we propose a general framework, UGNN, which enables the development of novel and flexible GNN models from the denoising perspective via regularizer design. As an example demonstrating the promise of this paradigm, we instantiate the UGNN framework with a regularizer addressing adaptive local smoothness across nodes, and proposed and evaluated a suitable new GNN model, ADA-UGNN.

ACKNOWLEDGEMENTS

This research is supported by the National Science Foundation (NSF) under grant numbers IIS1714741, CNS1815636, IIS1845081, IIS1907704, DRL2025244, IIS1928278, IIS1955285, IOS2107215, IOS2035472, Army Research Office (ARO) under grant number W911NF-21-1-0198, and a grant from Snap Inc.

REFERENCES

- [1] Joan Bruna, Wojciech Zaremba, Arthur Szlam, and Yann LeCun. 2013. Spectral networks and locally connected networks on graphs. *arXiv preprint arXiv:1312.6203* (2013).

- [2] Siheng Chen, Yonina C Eldar, and Lingxiao Zhao. 2020. Graph Unrolling Networks: Interpretable Neural Networks for Graph Signal Denoising. *arXiv preprint arXiv:2006.01301* (2020).
- [3] Siheng Chen, Aliaksei Sandryhaila, José MF Moura, and Jelena Kovacevic. 2014. Signal denoising on graphs via graph filtering. In *2014 IEEE Global Conference on Signal and Information Processing (GlobalSIP)*. IEEE, 872–876.
- [4] Eli Chien, Jianhao Peng, Pan Li, and Olgica Milenkovic. 2020. Adaptive universal generalized pagerank graph neural network. *arXiv preprint arXiv:2006.07988* (2020).
- [5] Gabriele Corso, Luca Cavalleri, Dominique Beaini, Pietro Liò, and Petar Veličković. 2020. Principal neighbourhood aggregation for graph nets. *arXiv preprint arXiv:2004.05718* (2020).
- [6] Michaël Defferrard, Xavier Bresson, and Pierre Vandergheynst. 2016. Convolutional neural networks on graphs with fast localized spectral filtering. In *Advances in neural information processing systems*. 3844–3852.
- [7] Guoji Fu, Yifan Hou, Jian Zhang, Kaili Ma, Barakeel Fanseu Kamhoua, and James Cheng. 2020. Understanding graph neural networks from graph signal denoising perspectives. *arXiv preprint arXiv:2006.04386* (2020).
- [8] Hongyang Gao, Zhengyang Wang, and Shuiwang Ji. 2018. Large-scale learnable graph convolutional networks. In *Proceedings of the 24th ACM SIGKDD*. 1416–1424.
- [9] Justin Gilmer, Samuel S Schoenholz, Patrick F Riley, Oriol Vinyals, and George E Dahl. 2017. Neural message passing for quantum chemistry. *arXiv preprint arXiv:1704.01212* (2017).
- [10] Will Hamilton, Zhitaoying, and Jure Leskovec. 2017. Inductive representation learning on large graphs. In *NeurIPS*. 1024–1034.
- [11] Mikael Henaff, Joan Bruna, and Yann LeCun. 2015. Deep convolutional networks on graph-structured data. *arXiv preprint arXiv:1506.05163* (2015).
- [12] Xiao Huang, Jundong Li, and Xia Hu. 2017. Label informed attributed network embedding. In *Proceedings of the Tenth ACM International Conference on Web Search and Data Mining*. 731–739.
- [13] Wei Jin, Yao Ma, Xiaorui Liu, Xianfeng Tang, Suhang Wang, and Jiliang Tang. 2020. Graph Structure Learning for Robust Graph Neural Networks. *arXiv preprint arXiv:2005.10203* (2020).
- [14] Thomas N Kipf and Max Welling. 2016. Semi-supervised classification with graph convolutional networks. *arXiv preprint arXiv:1609.02907* (2016).
- [15] Johannes Klicpera, Aleksandar Bojchevski, and Stephan Günnemann. 2018. Predict then propagate: Graph neural networks meet personalized pagerank. *arXiv preprint arXiv:1810.05997* (2018).
- [16] Yao Ma, Xiaorui Liu, Neil Shah, and Jiliang Tang. 2021. Is Homophily a Necessity for Graph Neural Networks? *arXiv preprint arXiv:2106.06134* (2021).
- [17] Yao Ma and Jiliang Tang. 2021. *Deep learning on graphs*. Cambridge University Press.
- [18] Federico Monti, Davide Boscaini, Jonathan Masci, Emanuele Rodola, Jan Svoboda, and Michael M Bronstein. 2017. Geometric deep learning on graphs and manifolds using mixture model cnns. In *Proceedings of the IEEE Conference on CVPR*. 5115–5124.
- [19] Hoang NT and Takanori Maehara. 2019. Revisiting graph neural networks: All we have is low-pass filters. *arXiv preprint arXiv:1905.09550* (2019).
- [20] Hongbin Pei, Bingzhe Wei, Kevin Chen-Chuan Chang, Yu Lei, and Bo Yang. 2020. Geom-gcn: Geometric graph convolutional networks. *arXiv preprint arXiv:2002.05287* (2020).
- [21] Yu Rong, Wenbing Huang, Tingyang Xu, and Junzhou Huang. 2019. Dropedge: Towards deep graph convolutional networks on node classification. In *International Conference on Learning Representations*.
- [22] Prithviraj Sen, Galileo Namata, Mustafa Bilgic, Lise Getoor, Brian Galligher, and Tina Eliassi-Rad. 2008. Collective classification in network data. *AI magazine* 29, 3 (2008), 93–93.
- [23] Neil Shah. 2020. Scale-Free, Attributed and Class-Assortative Graph Generation to Facilitate Introspection of Graph Neural Networks. *KDD Mining and Learning with Graphs* (2020).
- [24] Oleksandr Shchur, Maximilian Mumme, Aleksandar Bojchevski, and Stephan Günnemann. 2018. Pitfalls of graph neural network evaluation. *arXiv preprint arXiv:1811.05868* (2018).
- [25] David I Shuman, Sunil K Narang, Pascal Frossard, Antonio Ortega, and Pierre Vandergheynst. 2013. The emerging field of signal processing on graphs: Extending high-dimensional data analysis to networks and other irregular domains. *IEEE signal processing magazine* 30, 3 (2013), 83–98.
- [26] Ryan J Tibshirani et al. 2014. Adaptive piecewise polynomial estimation via trend filtering. *The Annals of Statistics* 42, 1 (2014), 285–323.
- [27] Petar Veličković, Guillem Cucurull, Arantxa Casanova, Adriana Romero, Pietro Liò, and Yoshua Bengio. 2017. Graph attention networks. *arXiv preprint arXiv:1710.10903* (2017).
- [28] Yu-Xiang Wang, James Sharpnack, Alexander J Smola, and Ryan J Tibshirani. 2016. Trend filtering on graphs. *The Journal of Machine Learning Research* 17, 1 (2016), 3651–3691.
- [29] Huijun Wu, Chen Wang, Yuriy Tyshetskiy, Andrew Docherty, Kai Lu, and Liming Zhu. 2019. Adversarial examples on graph data: Deep insights into attack and defense. *arXiv preprint arXiv:1903.01610* (2019).
- [30] Jun Wu, Jingrui He, and Jiejun Xu. 2019. Net: Degree-specific graph neural networks for node and graph classification. In *Proceedings of the 25th ACM SIGKDD International Conference on Knowledge Discovery & Data Mining*. 406–415.
- [31] Zhilin Yang, William Cohen, and Ruslan Salakhudinov. 2016. Revisiting semi-supervised learning with graph embeddings. In *International conference on machine learning*. PMLR, 40–48.
- [32] Rex Ying, Ruining He, Kaifeng Chen, Pong Eksombatchai, William L Hamilton, and Jure Leskovec. 2018. Graph convolutional neural networks for web-scale recommender systems. In *Proceedings of the 24th ACM SIGKDD*. 974–983.
- [33] Zhitaoying, Jiaxuan You, Christopher Morris, Xiang Ren, Will Hamilton, and Jure Leskovec. 2018. Hierarchical graph representation learning with differentiable pooling. In *Advances in neural information processing systems*. 4800–4810.
- [34] Lingxiao Zhao and Leman Akoglu. 2019. Pairnorm: Tackling oversmoothing in gnns. *arXiv preprint arXiv:1909.12223* (2019).
- [35] Tong Zhao, Yozen Liu, Leonardo Neves, Oliver Woodford, Meng Jiang, and Neil Shah. 2020. Data Augmentation for Graph Neural Networks. *arXiv preprint arXiv:2006.06830* (2020).
- [36] Jiong Zhu, Ryan A Rossi, Anup Rao, Tung Mai, Nedim Lipka, Nesreen K Ahmed, and Danai Koutra. 2020. Graph neural networks with heterophily. *arXiv preprint arXiv:2009.13566* (2020).
- [37] Jiong Zhu, Yujun Yan, Lingxiao Zhao, Mark Heimann, Leman Akoglu, and Danai Koutra. 2020. Beyond homophily in graph neural networks: Current limitations and effective designs. *arXiv preprint arXiv:2006.11468* (2020).
- [38] Meiqi Zhu, Xiao Wang, Chuan Shi, Houye Ji, and Peng Cui. 2021. Interpreting and Unifying Graph Neural Networks with An Optimization Framework. *arXiv preprint arXiv:2101.11859* (2021).
- [39] Daniel Zügner and Stephan Günnemann. 2019. Adversarial attacks on graph neural networks via meta learning. *arXiv preprint arXiv:1902.08412* (2019).